High resolution synchrotron radiation-based x-ray photoemission spectroscopy study of the Si-rich β-SiC(100) 3×2 surface oxidation

D. Dunham,[a),b)] S. Mehlberg, and S. Chamberlin
Department of Physics, University of Wisconsin-Eau Claire, Eau Claire, Wisconsin 54701

P. Soukiassian[a)]
Commissariat à l'Energie Atomique, Saclay, Laboratoire Surfaces et Interfaces de Matériaux Avancées associé à l'Université de Paris-Sud/Orsay, DSM-DRECAM-SPCSI, Batiment 462, 91191 Gif sur Yvette Cedex, France

J. D. Denlinger and E. Rotenberg
Advanced Light Source, Lawrence Berkeley National Laboratory, Berkeley, California 94720

B. P. Tonner
Department of Physics, University of Central Florida, Orlando, Florida 32816

Z. D. Hurych
Department of Physics, Northern Illinois University, DeKalb, Illinois 60115

(Received 24 January 2003; accepted 26 April 2003; published 5 August 2003)

We investigate the initial oxidation and interface formation of cubic silicon carbide for the silicon rich β-SiC(100) 3×2 surface reconstruction by high resolution synchrotron radiation-based soft x-ray photoemission spectroscopy. The surface is exposed to low doses of molecular oxygen ranging from 1 up to 10 000 L, at surface temperatures from 25 to 500 °C. Significant formation of SiO_2 is found for the surface at room temperature, with the rate of oxidation increasing with temperature. Valence band data and Si $2p$ core level spectra show that even at low exposures, significant oxidation is taking place, with a surface reactivity to oxygen much larger than for silicon surfaces. The oxidation products, which are grown at very low temperatures ($\leqslant$500 °C) include SiO_2 as a dominant feature but also substoichiometric oxides Si^{+1}, Si^{+2}, Si^{+3}, and significant amounts of mixed oxide products involving C atoms (Si–O–C). © *2003 American Vacuum Society.*
[DOI: 10.1116/1.1589515]

I. INTRODUCTION

Due to its very interesting properties, silicon carbide is expected to be a very suitable semiconductor for high-power, high-temperature, high-voltage, high-frequency, and radiation resistant electronics.[1–6] Recent progress in the growth of high-quality SiC wafers[6] have brought all these potential applications much closer to reality.[1–6] However, SiC has more than 170 different polytypes in hexagonal (α), cubic (β), and rhombohedric phases.[1–3] While cubic β-SiC has a smaller band gap than the hexagonal 4H and 6H-SiC polytypes, 2.4 eV instead of 3.3 and 2.9 eV, respectively, the mobilities are much higher with an average figure of merit scaling nearly one order of magnitude above those of hexagonal SiC.[5] While hexagonal SiC is more suitable for power electronic devices, β-SiC is especially suitable for high frequency devices for communication systems such as mobile phone power base stations.

One of the crucial issues that must be addressed during SiC device fabrication is the ability to produce high-quality SiO_2/SiC interfaces. Indeed, due to the exceptional properties of its native oxide, silicon dioxide is one of the major reasons why silicon is actually the most used semiconductor.[9–11] In addition to its exceptional properties, SiC also has SiO_2 as a native oxide. SiC exists in cubic (β-SiC) and hexagonal (α-SiC) structures and depending on the surface preparation and orientation this compound exhibits a wide variety of surface structure and composition. Thus investigations of the different clean surfaces and the effect of surface structure and composition on the initial oxidation is of central importance.

SiC oxidation has been investigated using various experimental techniques.[7–12] Hornetz *et al.*[12] have shown that oxidation of α-SiC surfaces is slower for the Si-terminated surface than for the C-terminated one and they suggested that this slower oxidation rate is related to the presence of a mixed $Si_4C_{4-x}O_2$ interface layer for the Si-terminated surface. In his x-ray photoemission study of oxygen adsorption on a different polytype surface, the cubic β-SiC(100), Bermudez[13] found a smaller initial O adsorption rate for the different SiC surfaces than for Si(100) and a strong resistance to the formation of SiO_2 on SiC. Recently, we have investigated that direct low molecular O_2 exposures on the Si-rich β-SiC(100) 3×2 and α-SiC(0001) 3×3 surface reconstructions lead to SiO_2 formation.[14–16]

In this article, we investigate the role of surface reconstruction on the β-SiC(100) oxidation using high-resolution core level photoemission spectroscopy with a third generation synchrotron radiation source (ALS, Berkeley). This third

[a)]Also at: Department of Physics, Northern Illinois University, DeKalb, IL 60115.
[b)]Electronic mail: dunhamdj@uwec.edu

generation source allows much higher energy resolution, especially when compared to previous work performed with x-ray sources,[12–14,17] allowing identification of oxidation states. The Si-rich 3×2 surface reconstruction exhibits Si–Si dimer rows, with all the dimers tilted in the same direction as evidenced by atom resolved scanning tunneling microscopy[18] and grazing incidence x-ray diffraction[19] and theory.[20] The oxidation is investigated at room temperature for various molecular oxygen exposures and at elevated temperatures up to 500 °C. While both the $2\times1/c(4\times2)$ and the 3×2 surfaces are both Si-terminated, Si-rich surfaces tend to be more reactive to oxygen.[21] In this article, we show that SiO_2/SiC interfaces could be achieved at much lower temperature than for silicon, with an interface having substoichiometric oxides and mixed oxide involving carbon atom products.

II. EXPERIMENTAL DETAILS

The experiments were performed on beam line 7.0.1 at the Advanced Light Source (ALS-LBNL, Berkeley, CA). The data were collected using an electrostatic PHI hemispherical electron analyzer with a mean radius of 150 mm. The acceptance angle of the analyzer was $\pm6°$. The overall energy resolution (monochromator+electron analyzer) was better than 60 meV at 150 eV photon energy used at the Si $2p$ core level and <100 meV at 340 eV photon energy used at the C $1s$ core level, which are probably the best energy resolutions ever used in investigating the SiC oxidation so far. We used both grazing and normal photoelectron emission which, combined with the tunability in energy of the synchrotron radiation, allows us to explore from the topmost atomic surface layer to the bulk sensitive regime. The pressure inside the experimental system was 1×10^{-10} Torr during data acquisition.

The sample was a cubic single domain SiC (β-SiC) thin film prepared by chemical vapor deposition of C_3H_8 and SiH_4 on a vicinal (4°) Si(100) wafer substrate at LETI (CEA-LETI, Grenoble). The surface quality was verified through sharp 3×2 low energy electron diffraction (LEED) patterns and by the lack of contamination related spectral features in the valence band and the core level spectra. Other details regarding the surface preparation of high quality β-SiC(100) 3×2 surfaces can be found elsewhere.[14,18,22]

The oxygen exposures were performed by leaking research grade oxygen into the chamber through a high-precision ultrahigh vacuum leak valve and by monitoring the pressure ($1\ \text{L}=1\times10^{-6}$ Torr s). The sample was heated by direct current flowing through the sample. The temperature was monitored using an optical pyrometer, using the emissivity of Si at 0.6, since SiC remains totally transparent.

III. RESULTS AND DISCUSSION

We first look at the initial oxidation process at room temperature for the β-SiC(100) 3×2 surface reconstruction by exploring the formation of oxidation products at silicon and carbon sites using the Si $2p$ and C $1s$ core levels. Figure 1(a) displays the Si $2p$ core level recorded at a 150 eV photon energy, for the clean and oxygen-exposed (1–10 000 L) 3×2 surface reconstruction. The energy scale is in relative binding energy with the origin at the Si $2p$ bulk component of SiC, located at 100.2 eV, i.e., at 1 eV higher binding energy compared to pure silicon (99.2 eV). The clean spectrum is shown with the peak decomposition involving three surface or subsurface components shifted to lower binding energy and one bulk component. The Si $2p$ peaks were fit using spin-orbit split Voigt functions. A Lorentzian width of 85 meV, a spin orbit splitting of 0.601 eV, and a branching ratio of 2:1 was used for all Si components. The full width at half maximum (FWHM) of the bulk component was 0.65 eV and each of the surface peaks had a FWHM of 0.51 eV. Upon O_2 exposure of 1 L, the Si $2p$ peak shape changes with components shifting to higher binding energy. At a 10 000 L oxygen exposure, a weak feature appears as a shoulder at a 2.8 eV relative binding energy, but starts to develop already in the lower exposure regimes. It corresponds to a small amount of silicon dioxide formation. The changing shape of the peak on the high binding energy side corresponds to lower oxidation states, indicating a nonabrupt insulator/SiC interface formation.

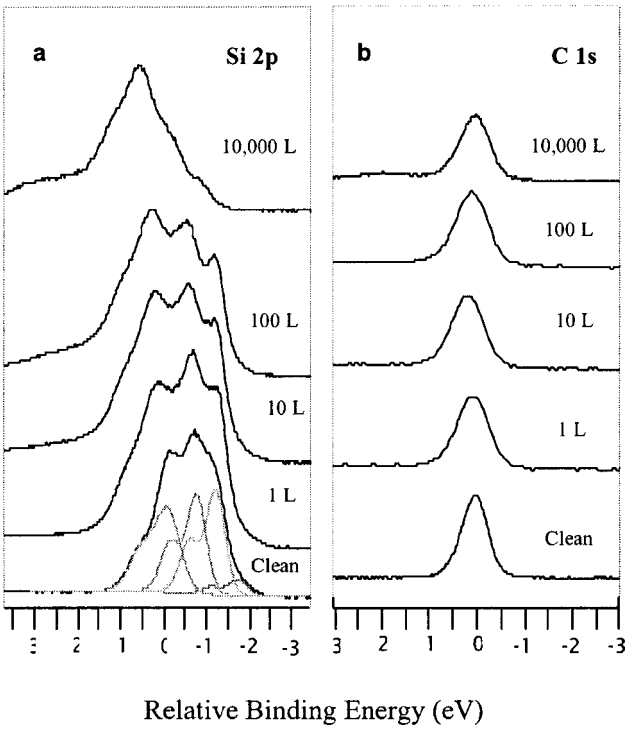

FIG. 1. Various molecular oxygen exposures at room temperature of the β-SiC(100) 3×2 surface: (a) Si $2p$ core levels ($h\nu=150$ eV, normal emission angle) and (b) C $1s$ core level ($h\nu=340$ eV, normal photoelectron emission). The binding energy scale is relative to the Si $2p$ (at 100.2 eV) and C $1s$ (at 281.6 eV) bulk component in silicon carbide.

Additional insights about oxygen interaction with the β-SiC(100) 3×2 surface reconstruction could be found by looking at the carbon atom environment using the C $1s$ core level. Figure 1(b) shows the C $1s$ core level line for the same oxygen exposure sequence as in Fig. 1(a). Unlike the Si $2p$ core level, oxygen exposure does not result in a chemical

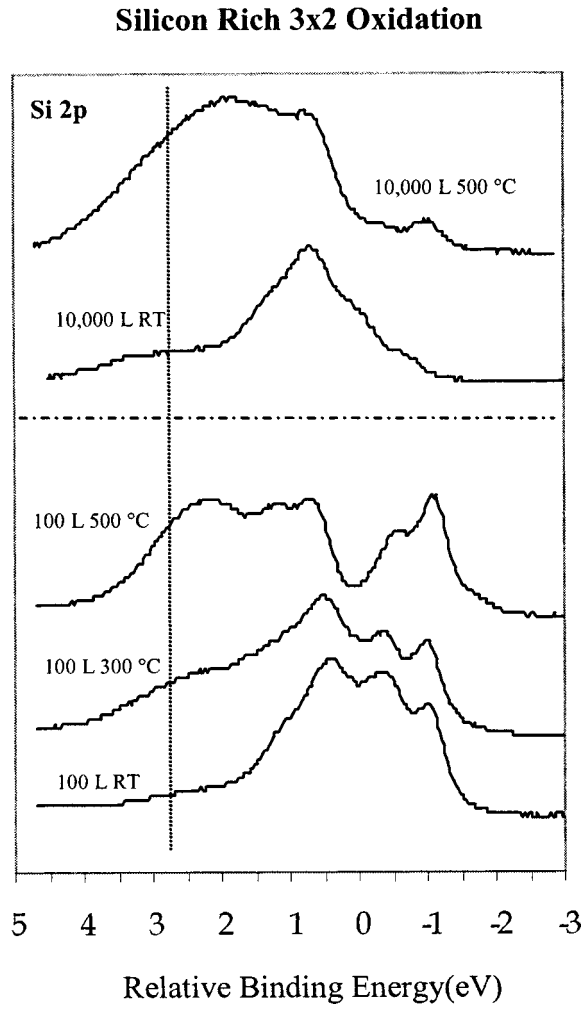

FIG. 2. Si 2*p* core level for the β-SiC(100) 3×2 surface oxidation at various molecular oxygen exposures at various temperatures between 25 and 500 °C for a photon energy of 150 eV. The binding energy scale is relative to the Si 2*p* bulk component in silicon carbide. The vertical line indicates the location of the Si^{+4} peak contribution.

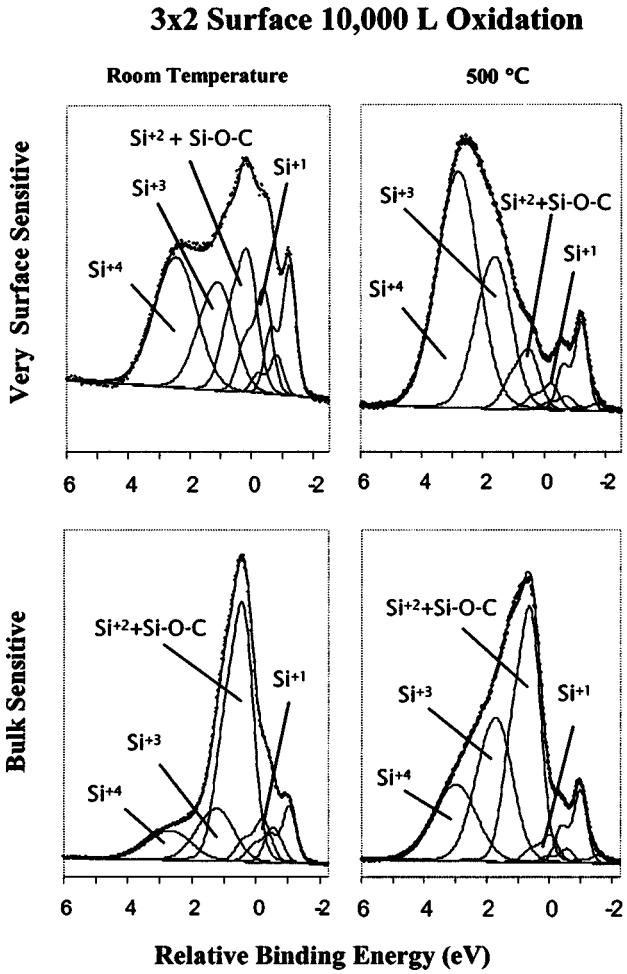

FIG. 3. 10 000 L of O_2 on a β-SiC(100) 3×2 surface at 25 and 500 °C. Decomposition of the Si 2*p* core level into chemically shifted components that are related to the Si oxidation states for very surface sensitive ($h\nu = 150$ eV and grazing photoelectron emission angle) and bulk sensitive ($h\nu = 340$ eV and normal emission photoelectron) spectra.

shifted component at the C 1*s* core level. However, one can notice that upon oxygen exposures the C 1*s* core level exhibits slight energy shifts associated with a significant broadening at the higher exposures (by approximately 15%) clearly indicating that the C atoms are involved in the oxidation process. This finding indicates that some of the silicon oxidation states most likely include mixed oxide products as Si–O–C. Actually, a similar situation has been observed for the Si-rich hexagonal 6H-/4H-SiC (0001) 3×3 surface reconstruction.[15,16]

We now look at the effect of temperature on the oxidation process for the 3×2 surface. The process can be followed by looking at the Si 2*p* core level for oxygen exposures of 100 L at 300 and 500 °C as shown at the bottom of Fig. 2, in a very surface sensitive mode for a 150 eV photon energy at normal photoelectron emission. Elevated temperatures have a much larger effect on the 3×2 surface oxidation process compared to extended oxygen exposures as can be seen in the Si 2*p* core levels. There is significant silicon dioxide formation for an exposure of 100 L at 300 °C. At 500 °C, the Si^{+4} peak becomes the dominant spectral feature of the oxidation products, together with two other spectral features that are related to substoichiometric oxides. When the oxygen exposure is increased to 10 000 L with a higher surface temperature of 500 °C, the amount of oxide products increases significantly as can be seen from the Si 2*p* core level displayed in the upper half of Fig. 2. This indicates that increasing temperatures facilitate oxygen insertion into the SiC lattice, most likely because temperature tends to increase the oxygen diffusion. Deeper insights about the various oxidation states of these products could be found using core level photoemission peak decomposition. Figure 3 displays decomposition of the Si 2*p* core level into chemical components for an oxygen exposure of 10 000 L at temperatures of 25 and 500 °C. The bottom set of spectra shows the decomposition for photon energy of 340 eV. The component peaks have a spin orbit splitting of 0.601 eV and a branching ratio of 2. The FWHMs are 1.3, 1.1, 0.9, and 0.60 eV for Si^{+4}, Si^{+3}, Si^{+2}, and Si^{+1}, respectively. Since the photoelectrons escape depth at higher kinetic energy is deeper, the corre-

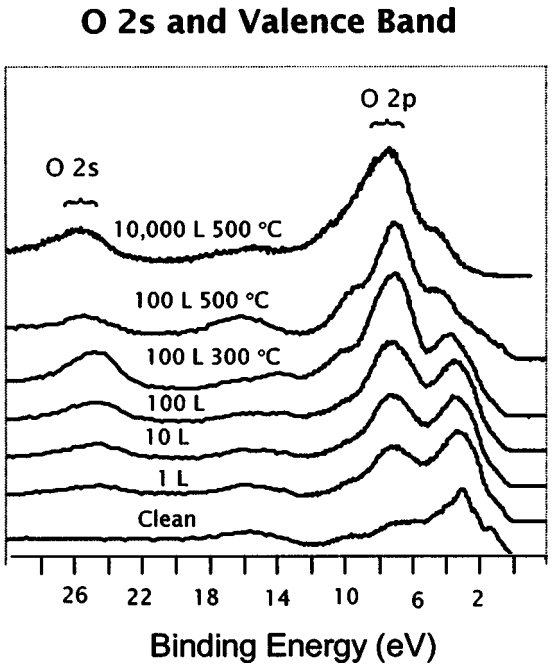

FIG. 4. Valence band photoemission spectra for O_2/β-SiC(100) 3×2 at various exposures and different temperatures ranging from 25 to 500 °C. The photon energy is 150 eV at normal emission angle.

sponding spectra are bulk sensitive especially at normal emission angle. At a photon energy of 150 eV, the photoelectron escape depth is about two to three atomic layers which, combined with a grazing emission angle, provide spectra very sensitive to the surface. In the spectra presented in Fig. 3, the peak located at about 2 eV relative binding energy indicates the formation of a Si^{+2} oxidation state. However, its intensity appears to be very large and it is likely resulting from mixed oxide products involving carbon atoms as Si–O–C with oxygen atoms bonded to both C and Si species as observed for hexagonal SiC.[14–17] Such an assignment is consistent with the C 1*s* broadening that is observed already at room temperature as also reported for the 6H-SiC(0001) 3×3 surface.[15,16] The top set of Si 2*p* spectra is recorded in the very surface sensitive mode at a 150 eV incident photon energy and at grazing emission. As surface sensitivity is increased, the contribution from the higher oxidation states increases indicating that the silicon dioxide is dominant on the surface with lower oxidation states located below it. These lower oxidation states even at higher temperatures indicate that the insulator–semiconductor interface is not abrupt.

The oxidation process can also be investigated by looking at the valence band spectra. Since the valence band electrons are the farthest out electrons in the atom, they are the most likely to show the oxygen uptake, especially at the lowest exposures. In Fig. 4, we see the valence band as a function of oxidation exposures from 1 to 100 L at room temperature and at 100 L at 300 and 500 °C and for 10 000 L at 500 °C. For the 3×2 surface, even at very low exposures like 1 L, we see a peak corresponding to the O 2*p* electrons and a small peak at the O 2*s* core level indicating that oxygen up-take is taking place already at this very low exposure regime. Indeed, the fact that these peaks become very pronounced already at very low exposures and room temperature indicates that the sticking probability of oxygen is very high on the β-SiC(100)3×2 surface, which is likely to explain why the oxidation is taking place at such low levels of oxygen. At elevated temperatures the oxygen signal becomes very large dominating the valence band spectra.

IV. CONCLUSIONS

The increased energy resolution available by third generation synchrotron radiation source based x-ray photoelectron spectroscopy now allows the identification of the different Si oxidation states of the β-SiC(100) surface. To summarize, our high resolution photoemission results have shown that the Si-rich β-SiC(100)3×2 surface is highly sensitive to oxygen, with SiO_2 formation already at room temperature. Elevated temperatures increase the amount of oxidation products leading to a SiO_2/SiC interface at rather low temperatures (<500 °C) which is known to provide oxides more resistant to radiation damages. However, carbon species are also involved in the oxidation products with the formation of small amounts of mixed Si–O–C oxides that remain located at the SiO_2/SiC interface.

ACKNOWLEDGMENTS

This work has been supported by the U.S. National Science Foundation through Northern Illinois University, NIU Graduate School Funds, and by the Office of Research and Sponsored Programs at UW-Eau Claire. Acknowledgment is also made to donors of the Petroleum Research Fund, administered by the American Chemical Society for partial support of this research. The authors are grateful to the Advanced Light Source at the Lawrence Berkeley National Laboratory for expert and outstanding technical assistance, and to L. di Ciccio, T. Billon, and C. Pudda (CEA-LETI, Grenoble) for providing high-quality cubic SiC thin films.

[1] *Silicon Carbide, A Review of Fundamental Questions and Applications to Current Device Technology*, edited by W. J. Choyke, H. M. Matsunami, and G. Pensl (Akademie Verlag, Berlin, 1998), Vols. I and II.
[2] *Properties of Silicon Carbide*, edited by G. Harris, EMIS Datareview Series (INSPEC, London, 1995), Vol. 13.
[3] *Silicon Carbide Electronics: Devices and Materials*, MRS Bull. **22** (1997).
[4] IEEE Trans. Electron Devices **46** (1999), and references therein.
[5] R. F. Davis, J. Vac. Sci. Technol. A **11**, 820 (1993).
[6] P. A. Ivanov and V. E. Chelnokov, Semiconductors **29**, 103 (1995).
[7] L. Simon, L. Kubler, A. Ermolieff, and T. Billon, Phys. Rev. B **60**, 5673 (1999).
[8] C. Virojanadara and L. I. Johansson, Surf. Sci. Lett. **472**, L145 (2001).
[9] S. Wolf and R. N. Tauber, *Silicon Processing for VLSI Era* (Lattice, Sunset Beach, CA, 1986).
[10] S. M. Sze, *Physics of Semiconductor Devices* (Wiley-Interscience, New York, 1981).
[11] M. Jaros, *Physics and Applications of Semiconductor Microstructures*, Oxford Science Publications, Series on Semiconductor Science and Technology 1 (Clarendon, Oxford, 1989).
[12] B. Hornetz, H. J. Michel, and J. Halbritter, J. Vac. Sci. Technol. A **13**, 767 (1995).

[13]V. M. Bermudez, J. Appl. Phys. **66**, 6084 (1989).
[14]F. Semond, L. Douillard, P. Soukiassian, D. Dunham, F. Amy, and S. Rivillon, Appl. Phys. Lett. **68**, 2144 (1996).
[15]F. Amy, P. Soukiassian, Y. K. Hwu, and C. Brylinski, Phys. Rev. B **65**, 165323 (2002).
[16]F. Amy, P. Soukiassian, Y. K. Hwu, and C. Brylinski, Appl. Phys. Lett. **75**, 3360 (1999).
[17]M. Riehl-Chudoba, P. Soukiassian, C. Jaussaud, and S. Dupont, Phys. Rev. B **51**, 14300 (1995).
[18]F. Semond, P. Soukiassian, A. Mayne, G. Dujardin, L. Douillard, and C. Jaussaud, Phys. Rev. Lett. **77**, 907 (1997).
[19]H. Enriquez, M. D'Angelo, V. Yu. Ariztov, P. Soukiassian, G. Renaud, A. Barbier, S. Chiang, and F. Semond, J. Vac. Sci. Technol. B, these proceedings.
[20]W. C. Lu, P. Kruger, and J. Pollman, Phys. Rev. B **60**, 2495 (1999).
[21]P. Soukiassian, in *Fundamental Aspects of Ultrathin Dielectrics on Si-based Devices: Towards and Atomic Scale Understanding*, edited by E. Garfunkel (Kluwer Academic, Dordrecht, Netherlands, 1998), p. 257.
[22]F. Semond, Ph.D. ™hesis, Université de Paris-Sud/Orsay, 1996.